Heliyon 9 (2023) e17214

Contents lists available at ScienceDirect

Heliyon

journal homepage: www.cell.com/heliyon

A comparative study of establishing rabbit vertebral tumor model by two ways of CT-guided percutaneous puncture

Zhilong Wang, Taiyang Zuo *, Wenli Lin, Yining Liang, Fangzhou Jiang, Yibing Li

Department of Oncology Intervention, Central Hospital Affiliated to Shandong First Medical University, 105 Jiefang Road, Jinan, Shangdong Province 250013, China

ARTICLE INFO

Keywords:
Microwave ablation
Vertebroplasty
VX2
Rabbit vertebral tumor model

ABSTRACT

Objective: To investigate the difference of tumor formation rate of rabbit vertebral tumor model established by percutaneous injection of V×2 tumor tissue suspension and tumor mass under computed tomography (CT) guidance, and the imaging findings of CT, magnetic resonance images (MRI) and positron emission tomography with computed tomography (PET/CT) at 7 days, 14 days and 21 days after implantation, and preliminarily verify the safety and feasibility of microwave ablation (MWA), percutaneous vertebroplasty (PVP) and microwave ablation combined with percutaneous vertebroplasty (MWA + PVP) in rabbit VX2 vertebral tumor model.

Methods: Thirty healthy New Zealand rabbits were randomly allocated to tissue suspension group and tumor block group, with 15 rabbits for each group. The VX2 tumor block and mixed suspension were inoculated into the L5 vertebral body under CT-guided percutaneous puncture. The PET/CT, MRI and CT examinations were performed at 7, 14 and 21 days after implantation. Fisher exact probability test was used to compare the success rate of the two implantation methods and the tumor display rate at each time point of the three examination methods. Observe the paralysis of tumor-forming rabbits, and immediately perform MWA/PVP/MWA + PVP treatment according to groups after paralysis to verify the safety and feasibility of treatment.

Results: A total of 18 experimental rabbits were successfully modeled in two groups, of which the success rate was 26.6% (4/15) in tissue suspension group and 93.3% (14/15) in tumor block group, with statistically significant differences between two groups ($P < 0.01$). The tumor display rates by PET/CT, MRI and CT at each time point after implantation were: 83.3% (15/18), 16.6% (3/18), and 0% (0/18) at 7 days after implantation; 100% (18/18), 88.8% (16/18), and 11.1% (2/18) at 14 days after implantation; and 100% (18/18), 100% (18/18), 77.7% (14/18) at 21 days after implantation. The average paralysis time of 18 experimental rabbits successfully modeled was 24.44 ± 2.38 days, and MWA/PVP/MWA + PVP treatment was performed in groups immediately after paralysis. Except for 2 rabbits who died due to anesthesia overdose during anesthesia before treatment, the remaining 16 rabbits were successfully treated with MWA/PVP/MWA + PVP, and the technical success rate was 100% (16/16). In MWA group, one experimental rabbit was randomly selected and killed after ablation, and histopathological examination (H and E staining) was performed together with 2 experimental rabbits who died of anesthesia. The pathological changes before and after ablation were compared. The survival time of the remaining 15 experimental rabbits varied from 3 to 8 days after treatment.

* Corresponding author.
E-mail addresses: 596821305@qq.com (Z. Wang), zuotaiyang001@163.com, zty3296@zxyy.cn (T. Zuo), linwenli@yeah.net (W. Lin), lyning1999@163.com (Y. Liang), 2805681108@qq.com (F. Jiang), echokui@163.com (Y. Li).

https://doi.org/10.1016/j.heliyon.2023.e17214
Received 15 February 2023; Received in revised form 6 June 2023; Accepted 9 June 2023
Available online 17 June 2023

Conclusion: The success rate of establishing rabbit vertebral tumor model by injecting tumor masses under the CT-guided percutaneous puncture is high, and the following MWA and PVP treatment can be successfully conducted. PET/CT is the most sensitive method for early detection of tumor compared with MRI and CT. Spectral Presaturation with Inversion Recovery (SPIR) sequence can significantly improve the detection rate of smaller tumors by MRI and shorten the detection time.

1. Introduction

The common metastases of malignant tumors are spine. Patients always suffer from pain, neurospinal cord compression, mobility disorders, pathological fractures, paraplegia, etc., resulting in a significant decline in the quality of life of patients, which in turn reduces the survival rate of patients [1,2]. In recent years, various minimally invasive methods based on percutaneous puncture techniques have emerged for the treatment of malignant tumors of the spine, such as percutaneous vertebroplasty, radiofrequency ablation and microwave ablation [3]. Microwave ablation (MWA) uses high-frequency electromagnetic waves in the frequency range of 900~2450 MHz to generate high temperature (mainly by the rotation of polar molecules to generate heat) to induce coagulative necrosis of tumor cells in order to achieve the therapeutic purpose of eliminating tumor [4,5]. Microwave ablation (MWA) has higher ablation efficiency due to its faster heating, larger ablation range, and less influence from high impedance tissues such as bone tissue, which is theoretically more effective for bone metastases [4,6–8]. However, rapid ablation at high power can cause nerve damages [3,9]. Percutaneous vertebroplasty (PVP) is to inject bone cement (PMMA) into the diseased vertebral body to reconstruct the physiological curvature of the patient's spine under the guidance of imaging, so as to enhance the stability of the spine [10,11]. After more than 20 years of development, it has become a reliable method for the treatment of vertebral hemangioma, osteoporotic vertebral compression fracture and vertebral malignant tumor. Compared with surgery, minimally invasive interventional technique has the advantages of less difficulty and trauma, short operation time and rapid recovery, especially ablation combined with percutaneous vertebroplasty is a research hotspot in the treatment of spinal metastases in recent years.

Animal experimentation is an important way to explore the principle of ablation therapy, find the optimal parameters of ablation conditions, improve the curative efficacy, and explore new ideas of combined therapy. However, extensive basic animal studies must be conducted before the large-scale application of these new treatments, in order to further understand the therapeutic mechanisms and to test the safety and efficacy of these new treatments. Therefore, the establishment of a reproducible and stable spinal tumor model is necessary to perform the basic tests described above. VX2 tumor model has been widely used in a variety of therapeutic studies, including percutaneous ablation, transarterial and chemoembolization, drug therapy and comprehensive therapy of solid VX2 tumor models such as liver, kidney and lung [12–16]. In this study, CT-guided percutaneous injection of VX2 tumor tissue suspension and tumor mass was used to establish a rabbit spinal tumor model. The CT, MRI and PET examinations were also performed to compare the tumor display rate at each time point of the three examination methods and the success rate of the two implantation methods. The feasibility of MWA and percutaneous vertebroplasty (PVP) treatment were also examined.

2. Materials and methods

The study was approved by the Animal Research Committee of the hospital and was conducted in accordance with the guidelines of the International Committee for the Protection of Animals. A total of 30 healthy New Zealand white rabbits (weight 3–3.5 kg, 3–4 months old, half male and half female) were used (purchased from Jinan Xilingjiao Breeding Center, animal use permit number: SCXK (Lu) 2020 0004). Fasting for 8 h was required before each invasive operation or imaging examination, and general anesthesia was administered by intravenous injection (2% sodium pentobarbital, 1.5–2 ml/kg) into the rabbit's ear.

2.1. VX2 tumor preparation

Thigh tumor-bearing rabbits in subculturing were taken, and the rabbits were sacrificed by the ear vein after the thigh skin was prepared. The outer thigh was disinfected with iodophor, then the local skin was cut open, the subcutaneous tissue was bluntly separated, and the complete tumor mass was plucked out with a scalpel, followed by removal of excess blood vessels and necrotic tissue with dissecting forceps and ophthalmic scissors. The fish-like tumor tissue was placed in a beaker with saline, and then was cut into small tumor pellets of 1 mm^3 or 0.5 mm^3 with ophthalmic scissors, and then mixed the tumor pellets with sterile saline in a 1:1 ratio to obtain tumor tissue suspension. All the above operations were conducted under aseptic conditions.

2.2. VX2 tumor implantation

A random grouping was used to randomly allocate 30 healthy New Zealand white rabbits into Group A and Group B, with 15 rabbits in each group. Group A used tumor tissue suspension for implantation and Group B used tumor block for implantation. After 8 h of preoperative fasting, the rabbits were anesthetized intravenously at the margins of the ears, and the operative area was shaved. Then the rabbits were fixed in a supine position on the self-made operating table. A large-aperture CT scan was localized (Philips, Netherlands), and the largest level of the lumbar 5 vertebra was taken as the target puncture level. After the skin around the puncture

point was disinfected, a 17G tapered puncture needle (GALLINI Company, Italy) was used to puncture into the center of the vertebral body along the lateral posterior border of the vertebral body at the junction with the pedicle under CT guidance (Fig. 1A–C). In group A, 0.2 ml of suspension was injected with a 1 ml syringe, and in group B, 3 pieces of 1 mm^3 tumor blocks were injected with a needle core. Both groups were sealed with 1 cm-long strips of gelatin sponge (Jinling Pharmaceutical Company, Nanjing, China) to block the needle passage.

2.3. Validation and treatment of rabbit spinal VX2 tumor model

PET/CT (Discovery MI; GE Healthcare, USA), MRI (MRI; 3.0 T Verio MRI machine, Philips, Netherlands) and CT (Philips, Netherlands) were performed 7 days, 14 days, and 21 days after the inoculation in the two groups (If the tumor has been shown in the previous examination, the same examination will not be done subsequently). The tumor display rate at each time point of the three examination methods and the success rate of the implantation methods in the two groups were compared. The criteria for successful tumor display within the vertebral body are as follows: significant high signal of the mass on MRI images on T2WI SPIR sequences/ radionuclide concentration within the vertebral body on PET/CT images/significant bone destruction or osteolytic mixed osteogenic changes at the implantation site on CT. The tumor display rate is the ratio found in the imaging examination after the successful construction of the vertebral tumor model.

The natural paralysis of 18 successfully modeled experimental rabbits was observed and recorded, and they were randomly divided into MWA group, PVP group, and MWA + PVP group, with 6 rabbits in each group. The success rate of the technique was recorded to initially verify its operational feasibility.

2.4. Imaging examination

Large aperture CT (Philips, Netherlands) was used for CT scanning. The scanning parameters are as follows: tube voltage 120 kV (peak), tube current 200 mA, layer thickness 1 mm, pitch 1. MR imaging was performed using (MRI; 3.0 T Verio MRI machine, Philips, Netherlands) and knee joint coils. Sagittal and axial T1-weighted images (TR/TE,500/12 ms), sagittal and axial T2-weighted images (TR/TE,2000/75 ms), sagittal and axial T2-weighted SPIR fat suppression images (TR/TE,2000/75 ms) were obtained. Fasting was prescribed for 4 h before PET/CT, 18F-FDG was injected into rabbit ear vein (27.8MBq/kg), and fixed in prone position for PET/CT scanning (Discovery MI; GE Healthcare, USA) after 30–40min. The CT scan parameters were: tube voltage of 80 kV, tube current of 300 mA, scan speed of 39.8 mm/s, pitch of 1, weight-based protocol and acquisition time of 2 min per bed to obtain PET images. All PET images were reconstructed by using an iterative algorithm, with CT-based attenuation correction applied. Metabolic images from PET and anatomic images from CT were fused in a postprocessing workstation (AW VolumShare 4.7; GE Healthcare).

2.5. CT-guided MWA with PVP procedure

MWA process (Fig. 5A and B): Under the guidance of CT, a 17G puncture needle (GALLINI Company, Italy) was successfully punctured to the lesion, then the needle core was pulled out and the puncture trocar was inserted into the ablation needle (outer

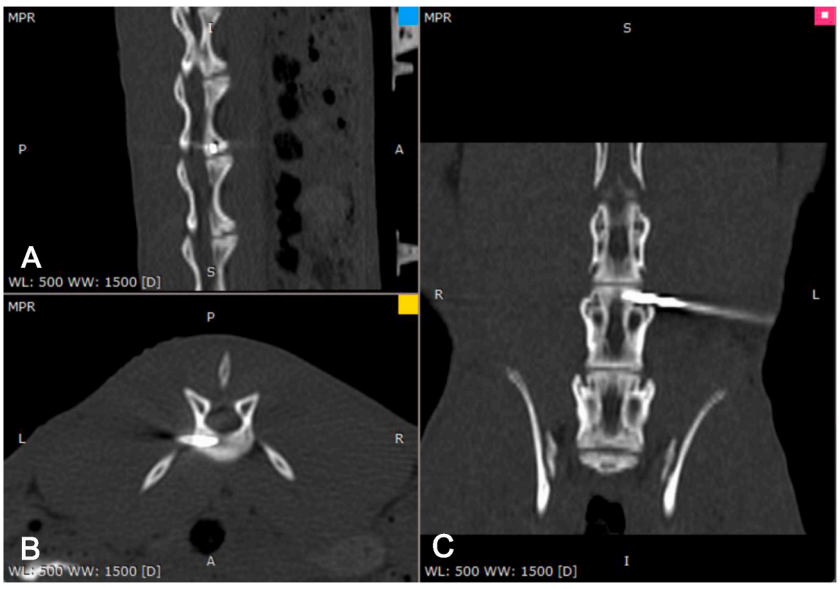

Fig. 1. The process of tumor implantation under CT guidance. A: sagittal view; B: axial view; C: coronal view, showing that the puncture needle enters the medullary cavity at the front end of the L5 vertebral body.

diameter 1.3 mm, length 11 cm; Yigao Microwave system Engineering Co., Ltd., Nanjing, China), and connected with the microwave ablation machine (ECO-100A1 microwave therapeutic instrument, Nanjing Yigao Microwave System Engineering Co., Ltd., microwave emission frequency is 2450 ± 20 MHz, output power: 0–150W, treatment time: 0 ~ 30min). The ablation parameters of 10W1min were used in MWA group, and those of 20W1min were used in MWA + PVP group. The microwave ablation needle was pulled out immediately after ablation, and the image was obtained after CT scanning, and the image performance was observed (after ablation, one experimental rabbit in MWA group was randomly selected and killed, and the histopathological examination was performed after dissection, Fig. 6A and B).

PVP procedure (Fig. 5C and D): Under the guidance of CT, a 17G puncture needle (GALLINI Company, Italy) was successfully punctured to the distal end of the ablated/non-ablated lesion. Bone cement (polymethylmethacrylate PMMA) (Heraeus Medical, Germany) was proportionally prepared and 0.3 ml of bone cement was slowly pushed into the vertebral body through a 1 ml syringe when the bone cement was in the "drawing phase", and the leakage of bone cement was observed (Experimental rabbits in the PVP group and the MWA + PVP group performed this step).

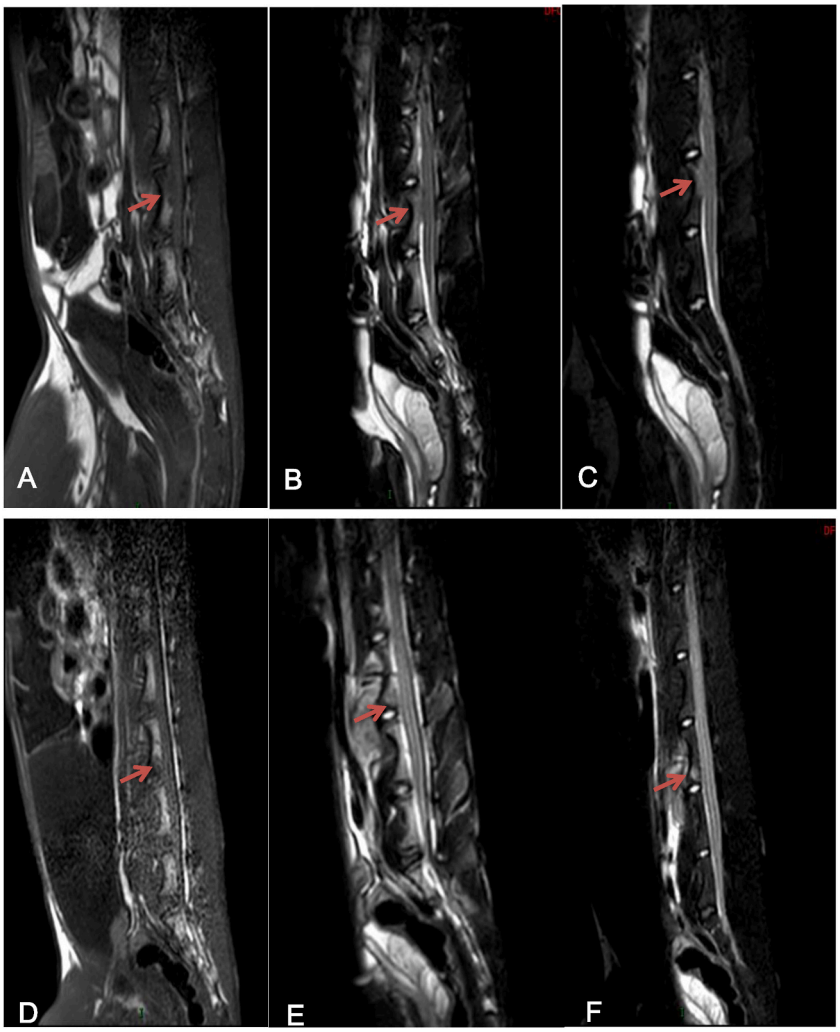

Fig. 2. MR images of L5 vertebra VX2 tumor model, A-C is an experimental rabbit with a large tumor 21 days after implantation, D-F is an experimental rabbit with a small tumor 14 days after implantation (The location of the tumor is shown by the red arrow). A: The mass shows long or slightly long signal changes on T1WI; B: The mass showed low and high mixed signal changes on the T2WI image, which was roughly equal to the normal bone marrow signal of the vertebral body. The difference between the two was not obvious, so the lesion was not clearly displayed; C: The mass is hyperintense on T2WI SPIR sequences, and the spinal cord is compressed; D & E: The mass is not clearly displayed on T1WI and T2WI; F: The mass showed obvious hyperintense signal on T2WI SPIR sequence and was confined to the medullary cavity. (For interpretation of the references to colour in this figure legend, the reader is referred to the Web version of this article.)

2.6. Statistical analysis

Statistical analysis was performed using SPSS 23.0 software. The counting data were expressed as percentage (%), and the continuous data were expressed as mean and standard deviation. Fisher's exact probability test was used for comparison between groups, and $P < 0.05$ was considered statistically significant.

3. Results

To compare the tumorigenic rate of the two implantation methods in the tumor model, the results showed the tumorigenic rate of the tissue suspension group was 26.6% (4/15) and the tumorigenic rate of the tumor block group was 93.3% (14/15). The difference between these two groups was statistically significant ($P < 0.01$). The tumor block group had a high rate of tumor formation and there was no extravertebral soft tissue tumor formation. The tumor display rates of PET/CT, MR and CT at each postoperative time were as follows (those had been shown for the first time by the same method were not followed up): 83.3% (15/18), 16.6% (3/18), and 0% (0/18) at 7 days after implantation; 100% (18/18), 88.8% (16/18), and 11.1% (2/18) at 14 days after implantation; 100% (18/18), 100% (18/18), and 77.7% (14/18) at 21 days after implantation. At 7 days after implantation, there was a statistically significant difference in the tumor display rate between PET/CT and MRI, PECT-CT and CT (both $P < 0.01$), but there was no significant difference in the tumor display rate between MRI and CT ($P > 0.05$). The difference in tumor display rate between CT and MRI, CT and PET/CT at 14 days after implantation were both statistically significant ($P < 0.01$), while the difference in tumor display rate between MRI and PET/CT was not statistically significant ($P > 0.05$). There was no statistically significant difference in tumor display rate between CT, MRI and PET/CT at 21 days after implantation ($P > 0.05$). MRI image at 7 days after implantation, most of the tumor signals are not obvious at this time, and it is difficult to determine whether the implantation is successful. MRI image at 14 days after implantation, at this time, the tumor is still small in size and mostly confined to the medullary cavity, but by this time, a significant signal contrast has been formed, which can clearly show the tumor (Fig. 2D–F). At 21 days after implantation, some of the larger tumors could break through the posterior edge of the vertebral body and invasion of the spinal cord could be seen (Fig. 2A–C). For PET/CT images, obvious radionuclide concentration could be seen in the vertebral body at 7 days after implantation (Fig. 3A and B). The appearance of PET/CT at 14 days after implantation was similar to that at 7 days after implantation, but the concentration area was enlarged and deepened. Although CT showed better bone destruction and osteogenic changes, it showed later. In most of the experimental rabbits in this study, 77.7% of the obvious bone changes appeared on CT 21 days after implantation (Fig. 4A–B), and some of them had not been clearly shown on CT at this time, which had been shown on MRI and PET/CT.

The average paralysis time of 18 experimental rabbits successfully modeled was 24.44 ± 2.38 days, and MWA/PVP/MWA + PVP treatment was performed in groups immediately after paralysis. Except for 2 rabbits who died due to anesthesia overdose during anesthesia before treatment, the remaining 16 rabbits were successfully treated with MWA/PVP/MWA + PVP, and the technical success rate was 100% (16/16). In MWA group, one experimental rabbit was randomly selected and killed after ablation, and histopathological examination (H and E staining) was performed together with 2 experimental rabbits who died of anesthesia. The pathological changes before and after ablation were compared. The survival time of the remaining 15 experimental rabbits varied from 3 to 8 days after treatment.

Compare the histopathological changes of vertebral tumors before and after ablation (hematoxylin and eosin, 10X). The pathological tumor cells of the non-ablated vertebral body grew diffusely without obvious necrosis; the tumor cells had large nuclei, deep staining, and little cytoplasm (Fig. 7A). Tumor coagulation necrosis with fragmented nuclei after ablation (Fig. 7B).

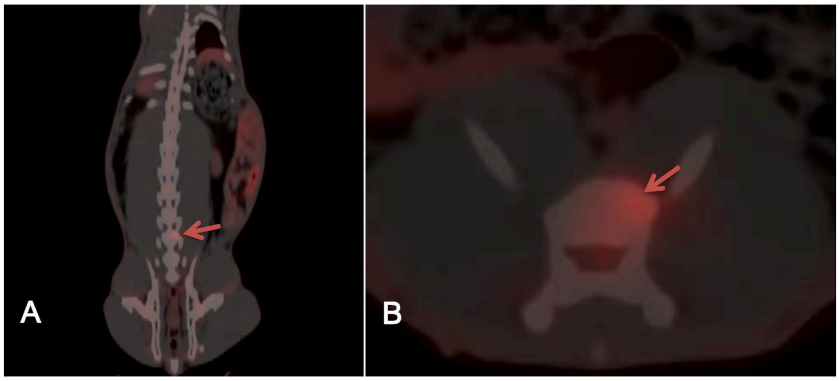

Fig. 3. 7 days after planting, PET-CT image of L5 vertebra VX2 tumor model, radionuclide concentration in the vertebral body (red arrow area). A: coronal view; B: axial view. (For interpretation of the references to colour in this figure legend, the reader is referred to the Web version of this article.)

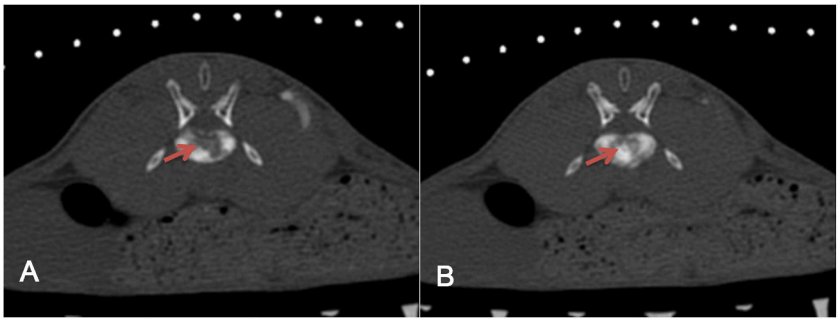

Fig. 4. 21 days after implantation, CT images of L5 vertebral body VX2 tumor model. A: Irregular bone destruction in the L5 vertebral body and cortical bone destruction at the posterior border of the vertebra (red arrow area); B: Osteogenic changes are seen inside the osteolytic changes (red arrow area). (For interpretation of the references to colour in this figure legend, the reader is referred to the Web version of this article.)

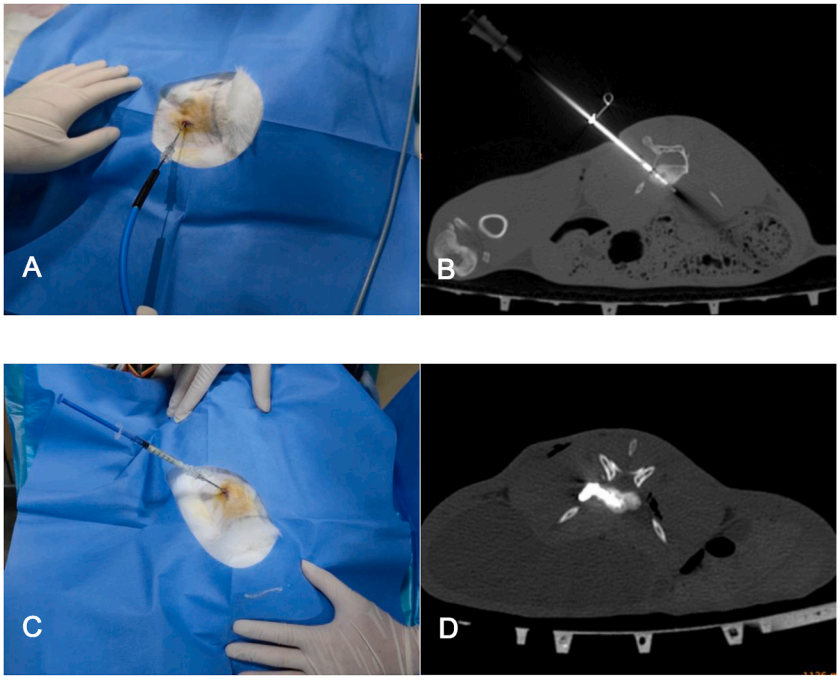

Fig. 5. Live imaging during microwave ablation and percutaneous vertebroplasty. A & B: Ablation schematic images; C & D: Bone cement injection images.

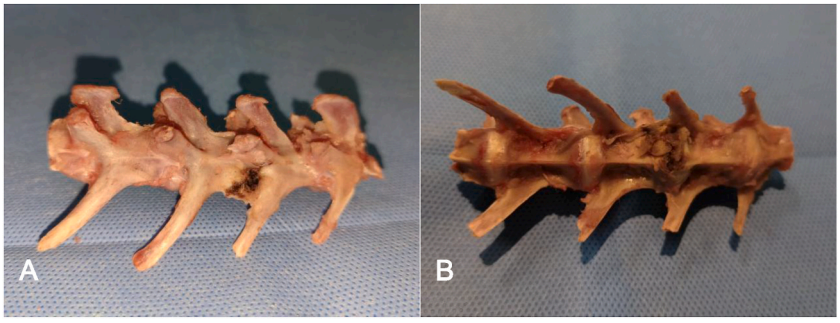

Fig. 6. Anatomical images of the spine after ablation. **A**: Carbonization is seen at the site of ablation; B: Destruction of cortical bone is seen at the site of tumor formation.

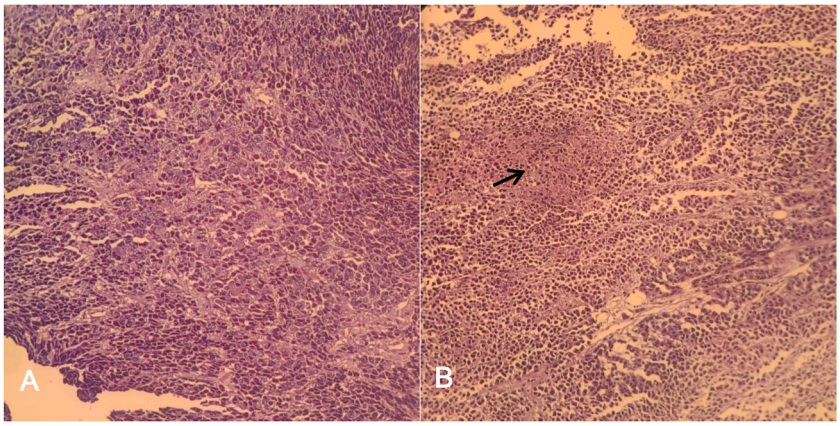

Fig. 7. **A:** The pathological tumor cells of the non-ablated vertebral body grew diffusely without obvious necrosis; the tumor cells had large nuclei, deep staining, and little cytoplasm; **B:** Tumor coagulation necrosis with fragmented nuclei after ablation (black arrow area).

4. Discussion

Currently, the commonly used animals for spinal model experiments mainly include rats, mice, nude mice and other rodents, as well as rabbits, dogs, and pigs [17]. However, due to the lack of plantable bone tumor cell lines in large experimental animals such as dogs and pigs, they are mostly used in the establishment of various bone injury models [18]. In addition, rodents, such as mice, have small vertebral bodies, so the tumor models produced are mostly used for basic research such as medicine, and are not suitable for research on interventional treatments such as surgery and ablation [18]. Rabbit VX2 tumor is a highly malignant squamous cell carcinoma characterized by rapid growth, vascular proliferation, and easy multiplication in skeletal muscle. Moreover, rabbit VX2 tumor has high similarity to human malignant tumor morphology and biological behavior, therefore, it is widely used in animal models for tumor treatment, and is an ideal animal model for simulating clinical studies of spinal metastasis [19,20].

Rabbit vertebral VX2 tumor models can be constructed by direct injection of tumor cell suspensions or by implantation of solid tumor blocks [21–24]. Amundson [22]and Masahito [21] successfully established an animal model of rabbit vertebral tumor by injecting VX2 tumor cell suspension/tumor block into the rabbit vertebral body under direct vision via a posterior dorsal approach exposing the vertebral arch. Although the above-mentioned methods of surgical inoculation have successfully established the VX2 vertebral tumor model in rabbits, the surgical incision method requires to incise and separate various layers of muscle fascia and other tissues, and attention must also be paid to protecting the position of the intervertebral foramen blood vessels and nerve roots, which requires high experimental skills and equipment. The operation time is also very long, and experimental animals suffer from relatively large trauma, which is not conducive to carrying out various treatment research on this model in the later stage. In addition, the surgical exposure of the vertebral body was followed by drilling and injecting the tumor block or suspension, which is not fundamentally different from the CT-guided puncture technique. Therefore, this study used CT-guided percutaneous puncture to establish a rabbit vertebral body tumor model.

The New Zealand rabbit lumbar spine is dumbbell-shaped, with the vertebral body height from L1-L7 showing the phenomenon of "large in the middle and small at both ends", and the L7 segment having the smallest vertebral body height while the L5 segment the largest. The width of the base of the vertebral body gradually increase from L1-L7, with the base of the L7 vertebral body being the widest. Since the L6 and L7 vertebral bodies are often covered by the pelvis, the L5 vertebral body is the best choice for implantation. However, CT-guided percutaneous puncture to establish a rabbit vertebral tumor model always requires high puncture technology. In the preliminary experiment of CT-guided percutaneous puncture in this study, it was found that rabbit vertebral bodies below 3 kg were too small, lacking obvious point of force during puncture. It is easy to slip from the vertebral body, and it is easy to damage the spinal canal when adjusting the direction of the puncture needle, while choosing experimental rabbits above 3 kg can significantly improve the success rate of puncture. Moreover, the 17G tapered puncture needle could implant the tumor block and gelatin sponge strip more smoothly, and its puncture needle cannula could be used as a channel for microwave ablation needle.

The tumor formation rate after implantation was 93.3% (14/15), while the success rate of implantation with tissue suspension was only 26.6% (4/15), which was much lower than that of Amundson's et al. study [22] (72% tumor formation rate after implantation). In Amundson's et al. study, VX2 tumor cell suspension was injected via surgical route to construct a vertebral VX2 tumor model. In this study, we concluded that unlike the surgical approach which uses direct vision to inject cell suspension and seal it with bone wax, it is more difficult to use fluid injection under imaging guidance. The bone marrow cavity in the rabbit vertebrae is small, it is difficult to accommodate enough fluid. Besides, the marrow cavity is relatively dense, when injected through a long needle, the pressure conduction can easily overflow the vertebral body, and only a small amount of fluid remains, so the tumor formation rate is low and easy to lead to paravertebral tumor formation. Comparatively, with tumor block implantation, the tumor volume can be easily controlled, the bone cortex is progressively destroyed, and extravasation is less likely to occur during implantation and cause peripheral implantation metastasis. Moreover, under the same circumstances, it is easier to successfully prepare models of the same size, which can homogeneously reflect the pathological changes of the transplanted rabbit VX2 vertebral tumor model. In this study, 1 case of tumor block

group failed to be implanted, and imaging examination showed paravertebral tumor formation. The author believes that the main reason for the paravertebral planting of the tumor in this case is that when pulling out the puncture needle after pushing the tumor block and sealing it with gelatin sponge, the tumor block that implanted closer to the edge was brought out along the way due to the puncture needle was more firmly embedded in the bone tissue.

In this study, PET/CT, MRI and CT examinations were performed on rabbits at 7, 14 and 21 days after implantation, and it was found that PET/CT performed at 7 days after implantation could detect the success of implantation at an early stage, and could clearly show whether the nuclear concentration area was in the vertebral body with the tumor display rate of 83.3% (15/18). While verification by MRI took two weeks to achieve a high display rate of 88.8% (16/18). Although CT showed better bone destruction and osteogenic changes, it was relatively late. In this study, obvious bone destruction did not appear on CT until day 21, and some of these changes had already been shown on MRI and PET/CT. Hu [25] et al. also found that PET/CT imaging using 18F-FDG tracer had higher sensitivity, accuracy and negative predictive value than MRI in the imaging diagnosis of spinal metastases in mice, which is consistent with the results of our study. However, according to Amundson [22] et al., MRI was unable to detect spinal tumors in experimental animals up to 14 days after implantation. In addition, Chen's [23] et al. study showed that only 3.5% (1/29) of vertebral body tumors were displayed by MRI on the 14th day after implantation, and 72.4% (21/29) were not displayed until 21 days after implantation. Differently, in this study, the MRI display rate of VX2 vertebral tumors in rabbits at the 2 nd week was 83.3% (15/18), and there were obvious signal differences in the normal bone marrow of vertebral bodies (Fig. 2A). However, on the T2WI image, there were low and high mixed signal changes, which were roughly equal to the normal bone marrow signal of the vertebral body, with no significant difference between them, so the lesion was not clearly displayed (Fig. 2B). SPIR (Spectral Presaturation with Inversion Recovery) sequence is a type of inversion recovery (IR) sequence, which can suppress 100% of the signal from adipose tissue and is currently one of the most sensitive and commonly used sequences in bone marrow examination. In this study, the rabbit VX2 vertebral tumor showed a high signal change on the SPIR image, and there was a significant signal difference between the normal bone marrow of the vertebra and the low signal, allowing the contour shape and destruction range of the lesion to be well displayed (Fig. 2C). The reason for the large tumor detection difference by MRI between our study and the above-mentioned study is that some of the tumors were still small at 14 days after implantation, and the low-signal hyposignal areas on T1WI images were not obvious, while the tumors themselves had small signal differences from normal bone marrow on T2WI images, so they were more difficult to be detected on T1WI and T2WI images. In contrast, the SPIR sequence was used in this study, and good display was obtained even for smaller tumors (Fig. 2F). This study concluded that the SPIR sequence could significantly improve the detection rate of smaller tumors by MRI and shorten the detection time.

Previous literatures have reported that the CT manifestations of the rabbit vertebral VX tumor model showed irregular osteolytic bone destruction in the vertebral body and/or pedicle [21,22]. In this study, we observed irregular osteogenesis around the bone destruction in addition to osteolytic bone destruction at the CT examination 21 days after implantation. We believe that the VX2 tumor strain is not only dominated by osteolytic destruction in the vertebral body, but also accompanied by an osteogenic growth pattern (Fig. 4A and B).

In this study, rabbits with successful implantation were treated with MWA and PVP. Due to the firmer rabbit bone cortex and smaller rabbit vertebral body, we chose a thinner ablation needle with a diameter of 1.3 mm during MWA, and a 17G puncture needle for the trocar. All tumor-bearing rabbits obtained technical approval, and preliminary results suggest that the operation is feasible. In addition, we found that the rabbits treated with MWA would go through a process of continuous improvement in physical status after treatment and finally continuous deterioration in physical status until death, and the improvement in physical status was the result of tumor killing by MWA.

The present study has some limitations. First, the number of experimental animals is relatively small. Second, the experimental rabbit vertebral body is small, which limits the selection of ablation power and ablation time. According to the size of the rabbit vertebral body, only two groups of ablation parameters, 10W 1min and 20W 1min, were tested in this study. Third, the purpose of this study for the treatment of MWA and PVP is only a preliminary test to accumulate experience for further experiments. The therapeutic effect of ablation has not been verified, and the rabbits were already paralyzed before treatment, so the impact of ablation on the nerves cannot be further tested.

5. Conclusion

In this study, VX2 tumors were inoculated by percutaneous puncture, and a vertebral tumor model suitable for percutaneous puncture was successfully established. The CT-guided percutaneous puncture method of injecting tumor blocks to establish a rabbit spinal tumor model has a high success rate and allows for successful next-step of MWA and PVP treatment. Compared with MRI and CT, PET/CT is the most sensitive method for early detection of tumor implantation. SPIR sequence can significantly improve the detection rate of MRI for smaller tumors and shorten the detection time. In the future experiments, we will further explore the relationship between the ablation range and MWA output power to help establish a more accurate ablation parameter standard, determine a relatively safe ablation time and power as well as a safe distance from the spinal cord, to lay the foundation for the popularization of MWA in the treatment of spinal tumors. In addition, testing the application of various thermometric and neuroprotective measures to reduce the complications of thermal injury may be one of the future research directions.

Author contribution statement

Zhilong wang: Conceived and designed the experiments; Performed the experiments; Analyzed and interpreted the data;

Contributed reagents, materials, analysis tools or data; Wrote the paper.

Taiyang Zuo: Conceived and designed the experiments; Performed the experiments; Analyzed and interpreted the data; Contributed reagents, materials, analysis tools or data..

Wenli Lin: Performed the experiments; Analyzed and interpreted the data; Contributed reagents, materials, analysis tools or data.;

Yining Liang: Fangzhou Jiang: Yibing Li: Performed the experiments; Contributed reagents, materials, analysis tools or data..

Funding statement

This work was supported by the project of Quancheng '5150' talent introduction and multiplication plan innovative talents, as well as Shandong Provincial Health Commission (No. 2019WS077).

Data availability statement

No data was used for the research described in the article.

Declaration of competing interest

The authors declare that they have no known competing financial interests or personal relationships that could have appeared to influence the work reported in this paper.

References

[1] D. Jiao, et al., Radiofrequency ablation versus 125I-seed brachytherapy for painful metastases involving the bone, Oncotarget 7 (52) (2016) 87523–87531.
[2] N. Gennaro, et al., Thermal ablation to relieve pain from metastatic bone disease: a systematic review, Skeletal Radiol. 48 (8) (2019) 1161–1169.
[3] A. Tomasian, et al., Percutaneous minimally invasive thermal ablation for management of osseous metastases: recent advances, Int. J. Hyperther. 36 (2) (2019) 3–12.
[4] M.A. Khan, et al., Efficacy and safety of percutaneous microwave ablation and cementoplasty in the treatment of painful spinal metastases and myeloma, AJNR Am. J. Neuroradiol. 39 (7) (2018) 1376–1383.
[5] K. Gala, et al., Microwave ablation: how we do it, Indian J. Radiol. Imag. 30 (2) (2020).
[6] S. Aubry, et al., Prospective 1-year follow-up pilot study of CT-guided microwave ablation in the treatment of bone and soft-tissue malignant tumours, Eur. Radiol. 27 (4) (2017) 1477–1485.
[7] B. Liu, et al., Safety and efficacy of microwave ablation for breast cancer thoracic metastases, Cancer Manag. Res. 10 (2018) 5685–5689.
[8] M.H. Wu, et al., Use of percutaneous microwave ablation for the treatment of bone tumors: a retrospective study of clinical outcomes in 47 patients, Cancer Imag. 19 (1) (2019) 87.
[9] A. Tomasian, et al., Vertebral metastases: minimally invasive percutaneous thermal ablation, Tech. Vasc. Intervent. Radiol. 23 (4) (2020), 100699.
[10] R. Ravikanth, Management of metastatic vertebral lesions by interventional techniques: systematic review of outcomes, J. Craniovertebral Junction Spine 11 (2) (2020) 61–70.
[11] Y. Yang, et al., Vessel-plasty using bone-filling mesh container for treatment of malignant severe compression fractures in cervical vertebrae, J. Pain Res. 15 (2022) 1173–1182.
[12] S.K. Yoon, et al., Radiofrequency ablation of renal VX2 tumors with and without renal artery occlusion in a rabbit model: feasibility, therapeutic efficacy, and safety, Cardiovasc. Intervent. Radiol. 32 (6) (2009) 1241–1246.
[13] A. Ueki, et al., Combination therapy involving radiofrequency ablation and targeted chemotherapy with bevacizumab plus paclitaxel and cisplatin in a rabbit VX2 lung tumor model, BMC Res. Notes 11 (1) (2018) 251.
[14] J. Chen, et al., The correlation between multimodal radiomics and pathology about thermal ablation lesion of rabbit lung VX2 tumor, Front. Oncol. 12 (2022), 941752.
[15] H. Zhang, et al., Renal and hepatic artery embolization with Pickering gel emulsion of lipiodol in rabbit, BMC Cancer 22 (1) (2022) 1300.
[16] Z. Zheng, et al., Idarubicin-loaded biodegradable microspheres enhance sensitivity to anti-PD1 immunotherapy in transcatheter arterial chemoembolization of hepatocellular carcinoma, Acta Biomater. 157 (2023) 337–351.
[17] D. Cossigny, et al., In vivo animal models of spinal metastasis, Cancer Metastasis Rev. 31 (1–2) (2012) 99–108.
[18] K. Zhang, et al., Application of hydroxyapatite nanoparticles in tumor-associated bone segmental defect, Sci. Adv. 5 (8) (2019), eaax6946.
[19] M.P. Melancon, et al., Development of an electroporation and nanoparticle-based therapeutic platform for bone metastases, Radiology 286 (1) (2018) 149–157.
[20] S.Y. Li, et al., Ultrasonic cavitation ameliorates antitumor efficacy of residual cancer after incomplete radiofrequency ablation in rabbit VX2 liver tumor model, Trans. Oncol. 12 (8) (2019) 1113–1121.
[21] M. Takahashi, et al., Experimental study of paraplegia caused by spinal tumors: an animal model of spinal tumors created by transplantation of VX2 carcinoma, Spine J. 4 (6) (2004) 675–680.
[22] E. Amundson, et al., A novel intravertebral tumor model in rabbits, Neurosurgery 57 (2) (2005) 341–346. ; discussion 341-346.
[23] L. Chen, et al., Establishing a rabbit spinal tumor model for nonvascular interventional therapy through CT-guided percutaneous puncture inoculation, AJNR Am. J. Neuroradiol. 36 (1) (2015) 153–159.
[24] Z. Yu, et al., Biomembrane formation after radiofrequency ablation prevents bone cement extravasation during percutaneous vertebroplasty for treating vertebral metastases with posterior margin destruction: an animal study, J. Cancer Res. Therapeut. 16 (5) (2020) 1082–1087.
[25] W. Hu, et al., Comparison of diagnostic efficacy of MRI and PET/CT in lung cancer of mouse with spinal metastasis, Cell. Mol. Biol. 66 (3) (2020) 138–142.